SPECTRAL ANALYSIS OF PRESSURE MEASUREMENTS OVER A MODIFIED BOEING BUMP

Nissrine Aziz
Department of Aerospace Engineering
The University of Illinois at Urbana-Champaign
104 S Wright St., Urbana, IL 61801
aziz7@illinois.edu

Theresa Saxton-Fox
Department of Aerospace Engineering
The University of Illinois at Urbana-Champaign
104 S Wright St., Urbana, IL 61801
tsaxtonf@illinois.edu

ABSTRACT

Time-resolved pressure measurements were analyzed using spectral analysis. This study aims to investigate critical phenomena in flow separation over a bump with a ratio of bump height to boundary layer thickness (h/δ) between 1 and 1.4 at different Reynolds numbers based on bump height (Re_h) ranging from 2.8×10^4 to 8.8×10^4. In this present work, spectral analysis was evaluated for a deeper understanding of the various fluid dynamics phenomena often detected in a separated flow over a modified Boeing bump. These fluid dynamics phenomena are often divided into three regions; breathing or flapping, vortex shedding and small-scale turbulence. Breathing or flapping at low-frequency of large coherent structure unsteadiness is associated with the expansion and contraction of the turbulent separation bubble (TSB) or the flapping of separated shear layer. This first region has been identified at Strouhal number $St_{Lsep} \approx 0.07-0.4$. A second region representative of vortex shedding at medium frequencies was identified at $St_{Lsep} > 0.4$. Small-scale turbulence at high frequency unsteadiness region was detected indicating the break down of the large shear layers due to Kelvin-Helmoltz instability. The interpretation of the low and medium frequencies origin is still ambiguous and requires extensive exploration in separated flow. With increased insight of the physics of separation, new strategies could be incorporated to mitigate flow separation.

INTRODUCTION

Turbulent boundary layer (TBL) separation is a critical fluid dynamic phenomenon that has been a topic of interest in various computational and experimental studies. Flow separation leads to an increase in drag over aircraft, automobile and ships. A strong adverse pressure gradient (APG) leads to TBL separation along the surface of a body leading to further aerodynamics implications. A TSB occurs when the TBL detaches from the surface of the geometry and reattaches further downstream creating a bubble as the name implies. Low-frequency coherent structures have been the center of attention to better understand complicated flow dynamics over different geometries Manohar *et al.* (2026); Steinfurth *et al.* (2024); Fang & Wang (2024); Steinfurth *et al.* (2025); Chen *et al.* (2024).

Flow separation has been studied over distinct geometries including the three dimensional Boeing Gaussian bump by Williams *et al.* (2021), the BeVERLI hill (Duetsch-Patel *et al.* (2022)) and the FAITH hill (Bell *et al.* (2012)). These investigations provide different flow conditions like Reynolds number and aspect ratio to compare distinct observations of TBL separation leading to a deeper understanding of the intriguing physics hidden behind flow separation phenomena. A range of important frequencies have been highlighted at medium and low frequencies. Very low frequencies, $St < 1\times10^{-3}$ have been reported by some researchers on Boeing bumps Manohar *et al.* (2026) and the Ahmed body Chen *et al.* (2024) marking an exhibit of bi-stable behavior. Low frequencies, at $St < 0.05$, have been observed in several studies, including on Boeing bumps and backward-facing ramps Klopsch *et al.* (2025); Steinfurth *et al.* (2025). Manohar *et al.* (2026) captures low-frequency unsteadiness at $St = 0.068$. But other studies on Boeing bumps have not shown evidence of such low frequency activity Williams *et al.* (2022).

Many studies have found medium-frequency spectral content, with $0.1 \leq St \leq 1$, with the exact bounds varying from study-to-study, along with the exact definition of the Strouhal number. These medium frequency regions were observed on Boeing bumps Williams *et al.* (2022); Klopsch *et al.* (2025), pressure-induced separation Mohammed-Taifour & Weiss (2016); Fang & Wang (2024), airfoils Floc'h *et al.* (2024), and ramps Steinfurth *et al.* (2025). These medium-frequency ranges are associated with vortex shedding in the separated region Eaton & Johnston (1982); Weiss *et al.* (2015). Open questions include the extent to which these low- and medium-frequency motions are geometry dependent, and if so, on which length scale(s) they scale, and whether they are Reynolds number dependent. The present work uses a modification to a Boeing bump that has a different aspect ratio to move towards clarification on the spanwise and streamwise length scales that may affect the low- and medium-frequency motions. This manuscript explores the presence of low, medium and high frequency unsteadiness regions associated to major flow dynamics phenomena that occur during flow separation.

EXPERIMENTAL METHODS

The modified Gaussian Boeing bump design, shown in figure 1, features three removable inserts to conduct high-frequency pressure and wall shear stress measurements, and will be used for future flow control testing to mitigate flow separation. The bump is Gaussian in the streamwise direction and tapered towards the wall; the flow was characterized in (Aziz *et al.* (2026)). The same equation 1 of the original Gaussian Boeing speed bump geometry that has been used by (Gray *et al.* (2021); Rizzetta & Garmann (2023); Gray *et al.* (2022)) is modified here to accommodate desired experimental techniques. The original bump has been modified to have two flat regions on the upstream and downstream sides to implement proper inserts for various forces measurements.
The original bump equation 1 has a Gaussian distribution with a height profile represented as y_G that varies with the streamwise coordinate x_b and the spanwise coordinate z_b, with an error function. The breadth and the steepness of the bump profile is defined as $x_0 = 0.225L$ and $z_0 = 0.06L$. Equation 2 represents the modified equation where y_b represents the bump profile height with $y_b = y_G$ between $|x| < x_1$ and $|x| > x_2$. The bump geometry was modified in the region $x_1 < |x| < x_2$ introducing a linear relationship between x and y_b. D represents the slope of the linear region with x, the linear region extends from $x_1 = 0.08$ to $x_2 = 0.12$. The same flat region is mirrored to the upstream region $-x_2 < |x| < -x_1$ but with a $-D$ slope.

$$y_G(x,z) = \frac{h}{2}\exp(-(x/x_0)^2)\left\{1+\operatorname{erf}\left[\left(\frac{L}{2}-2z_0-|z|\right)/z_0\right]\right\} \tag{1}$$

$$y_b(x,z) = \frac{h}{2}\left\{1+\operatorname{erf}\left[\left(\frac{L}{2}-2z_0-|z|\right)/z_0\right]\right\}(D(x-x_1)+y_G(x_1,z)) \tag{2}$$

Experiments were executed in a subsonic turbulent boundary layer wind tunnel at the University of Illinois at Urbana-Champaign within a test section that has a cross-sectional area of 0.381 × 0.381 m^2 and is 3.657 m long. The TBL evolves for 2.35 m over a flat plate before reaching the bump placed in the test section. Table 1 summarizes flow testing parameters, the freestream velocity (U_∞), the Reynolds number based on the bump height (Re_h) and the sampling time (T_s) for pressure measurements. $T_s = L/(St \cdot U_\infty)$ was identified using a Strouhal number of $St = 10^{-3}$ reported previously in flow separation region by (Williams & Smits (2025)). L represents the width of the bump in the spanwise direction with $L = 0.381$ m and h represents the maximum height of the bump where $h = 0.15L$. The height of the bump represents 19.3 % of the distance between the flat plate top surface and the ceiling of the wind tunnel.
Time-resolved pressure measurements on the downstream sides of the bump were taken using Kulite XCQ-093 with 30 kHz temporal resolution and a sensitivity of 20 mV/ psi. Four Kulites are shown in figure 1 mounted on the upstream side of the bump and flush with the surface. The sensors were placed at one streamwise position of x/L = 0.25 and four spanwise positions symmetrically spaced in respect to the center of the bump with 45 mm distance between each Kulite.

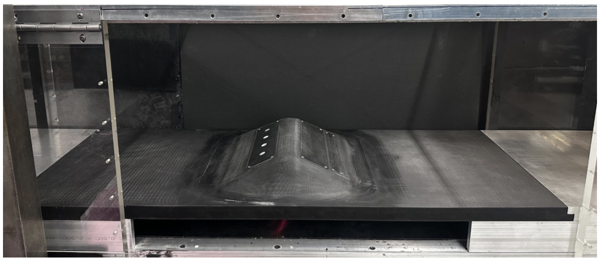

Figure 1: Modified Boeing bump.

Table 1: Experimental flow parameters.

Test	1	2	3
U_∞	7.7	19.6	24.2
$Re_h \times 10^4$	2.8	7.1	8.8
T_s (s)	50	20	16

RESULTS AND DISCUSSION

Welch's method was used to estimate the power spectral density (PSD) of time-resolved pressure measurements. The number of samples per segment known as *nperseg* was set to two different values depending on the frequencies we are interested in analyzing, a 50 % overlap was chosen and a Hamming windowing was used.
The pressure measurements from the downstream side of the bump at the single x-location and four z-locations were processed using the Welch's method. Long time signals were measured to enable the study of low Strouhal numbers, which are defined here in terms of an estimated separation length, which here is taken as $L_{sep} \equiv L/3$ Mabey (1972); Annamalai (2022). Welch's method requires binning the time signal into distinct regions in order to separately estimate their spectral content and average, to reduce noise. The number of samples used per segment was varied to enable the study of different frequencies: 2^{15} was used for the lower and medium frequencies while 2^{11} was used for the higher frequencies to reduce noise.

The results of the spectral content of time-resolved pressure measurements are shown in figures 2 and 3. The y-axis represents the PSD of the time-resolved pressure measurements in the separated region of the bump and the x-axis represents the Strouhal number St_{Lsep} normalized by the separation length. Figure 2 represents the spectral content using $nperseg = 2^{15}$ where each of the figures 2a, 2b and 2c represent the spectra of $U_\infty = 7.7, 19.6$ and 24.2 m/s respectively. Figure 3 shows the spectral content using $nperseg = 2^{11}$, where figures 3a, 3b and 3c represent the spectra of $U_\infty = 7.7, 19.6$ and 24.2 m/s respectively for all three flow conditions mentioned in table 1. For all three freestream velocities plotted in figure 2, low and medium frequency regions were identified.

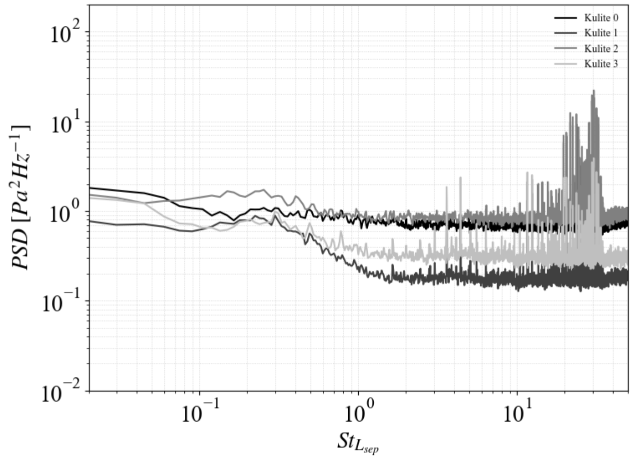

(a) $U_\infty = 7.7$ m/s

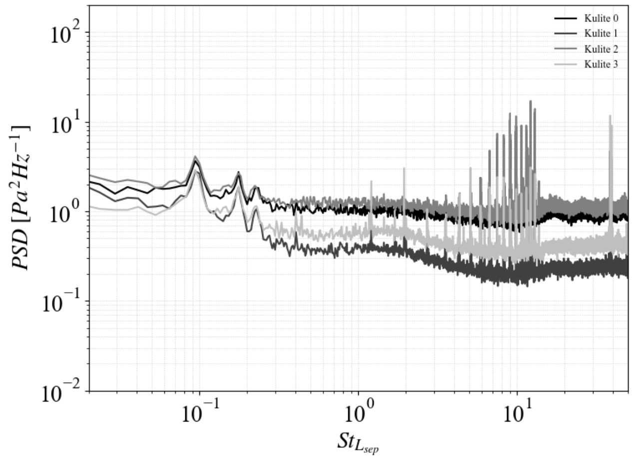

(b) $U_\infty = 19.6$ m/s

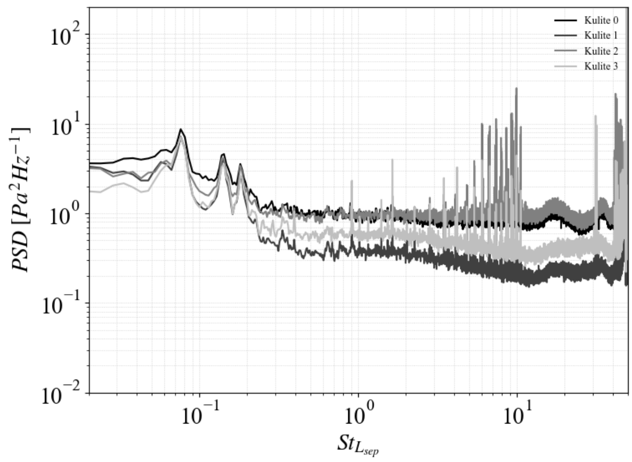

(c) $U_\infty = 24.2$ m/s

Figure 2: PSD for 2^{15} samples per segment

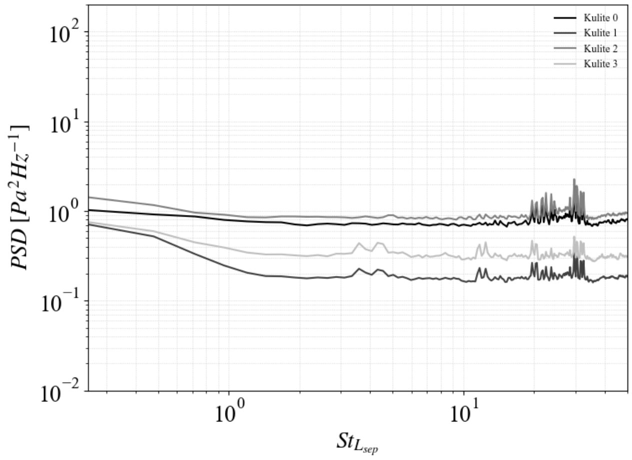

(a) $U_\infty = 7.7$ m/s

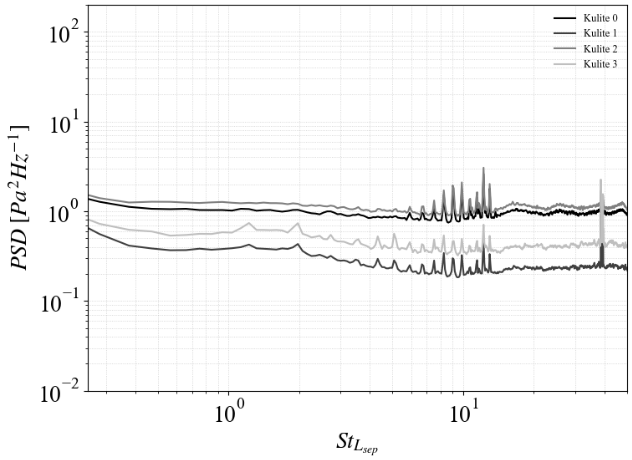

(b) $U_\infty = 19.6$ m/s

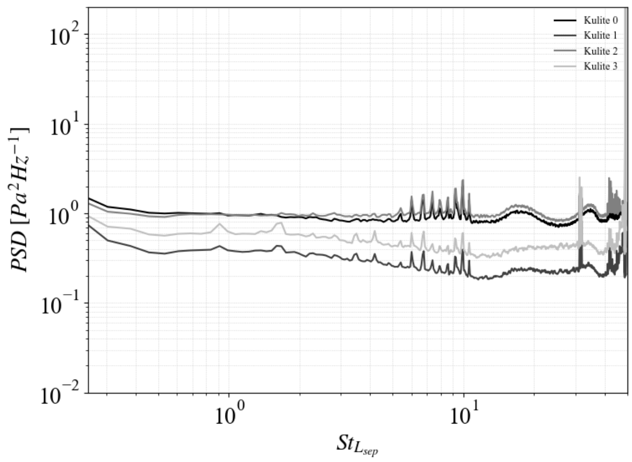

(c) $U_\infty = 24.2$ m/s

Figure 3: PSD for 2^{11} samples per segment

In the figures with $nperseg = 2^{15}$ (figures 2a, 2b and 2c), peaks are observed in the ranges $St_{L_{sep}} \approx 0.07 - 0.4$, with maintained high energy in the very low frequencies ($St_{L_{sep}} < 0.07$ but without distinct peaks. In the two cases with higher velocity, strong peaks are observed at $St_{Lsep} = 0.094$, $f = 14.65$ Hz and $St_{Lsep} = 0.076$, $f = 14.44$ Hz. Two additional peaks immediately follow at $St_{Lsep} = 0.18$ at $f = 28.1$ Hz and $St_{Lsep} = 0.23$ at $f = 35.85$ for the $U_\infty = 19.6$ m/s and $St_{Lsep} = 0.14$ at $f = 26.95$ Hz and the second one is located about $St_{Lsep} = 0.18$ at $f = 34.65$ for the $U_\infty = 24.2$ m/s cases. We can observe that these three peaks are related in their frequency content. We observe that the second peak is approximately twice the first peak, and that the third peak is approximately the sum of the first two. We therefore suggest that these three peaks all represent the same fundamental dynamics, with the harmonic and triadic relationship highlighting that they likely are collectively representing the skewness of the underlying coherent structure Manthripragada & Saxton-Fox (2024); Duvvuri & McKeon (2015). There is also a smaller and smoother hump near $St_{L_{sep}} \approx 1$. Very low frequency content is observed, suggesting that there is a very slow variation in the separation region leading to a very slow variation in the pressure at the surface of the bump.

The frequency content observed is consistent with prior studies on three-dimensional Gaussian bumps, though the present bump has a slighty different geometry than the traditional Boeing speed bump. Manohar *et al.* (2023) identified a peak at $St = 0.07$, $f = 13.5$ Hz, which they associated with the breathing motion or flapping of the separated shear layer. They also identified a motion at $f = 20$ Hz, which they associated with vortex shedding of the lateral shear layers Manohar *et al.* (2026). A higher Strouhal number of 0.68, $f = 135$ to 200 Hz was identified by Manohar *et al.* (2026) as the centerline shear-layer shedding; this observation represents large-scales coherent structures amalgamation and is often detected in separated flows due to Kelvin-Helmoltz instability Cherry *et al.* (1984).

We also note that the choice of Strouhal number that is used in figure 2 does not lead to a collapse in the Strouhal number associated with peaks as the Reynolds number is change. The Reynolds number dependence may indicate that the separation bubble length is a strong function of Reynolds number, which was observed for a similar bump in prior studies Borra (2024). Future work will include particle image velocimetry to study the size of the separation bubble.

CONCLUSION

We inspected the frequency content and spanwise-variability of the pressure to look for signatures of the breathing, vortex shedding, and small-scale turbulent activity in the separated region located downstream of a three-dimensional bump. Very low-frequency was detected around $St_{Lsep} = 0.006$ requiring further analysis to determine its underlying mechanism responsible of this behavior. A breathing or flapping region was identified at $St_{Lsep} \approx 0.07 - 0.4$ with dominant peaks at $St_{Lsep} = 0.094$, $St_{Lsep} = 0.18$ and $St_{Lsep} = 0.23$ for the $U_\infty = 19.6$ m/s case and $St_{Lsep} = 0.076$, $St_{Lsep} = 0.14$ and $St_{Lsep} = 0.18$ for the $U_\infty = 24.2$ m/s case. A vortex shedding region was identified at $St_{Lsep} > 0.4$. Small-scales turbulence structure at $St_{Lsep} \geq 1$ was identified over a larger frequency range with no prominent peaks. We compared the frequency content observed on this geometry to those of previously studied bumps and geometries to understand the relationship between geometry and separation frequency content. We found that low and medium frequencies are present and significantly more energetic with a higher spectral energy as the freestream velocity increases from 7.7 m/s to 24.2 m/s.
Further studies aim to implement spectral proper orthogonal decomposition (SPOD) to extract coherent structures at specific frequencies we are interested in to farther expand our investigation. Particle image velocimetry (PIV) will allow us to capture and analyze large scale coherent structure that are highly crucial and have been the main topic of interest for many in the fluid dynamics community.

ACKNOWLEDGMENTS

The support of the Air Force Office of Scientific Research through grant FA9550-23-1-0299 and the Office of Naval Research N00014-25-1-2255 is gratefully acknowledged.

REFERENCES

Annamalai, Hariprasad 2022 *Detailed characterization of turbulent separated flow dynamics and boundary layer evolution over a speed-bump geometry*. University of Washington.

Aziz, Nissrine, Mattei, Marco & Saxton-Fox, Theresa 2026 Flow characterization over a modified boeing bump. In *AIAA SCITECH 2026 Forum*, p. 0960.

Bell, James, Heineck, James, Zilliac, Greg, Mehta, Rabindra & Long, Kurt 2012 Surface and flow field measurements on the faith hill model. In *50th aiaa aerospace sciences meeting including the new horizons forum and aerospace exposition*, p. 704.

Borra, Akhileshwar 2024 Turbulent boundary layer separation and its driving factors. PhD thesis, University of Illinois at Urbana-Champaign.

Chen, CW, Wang, Sen & Ghaemi, S 2024 Spectral proper orthogonal decomposition of time-resolved three-dimensional flow measurements in the turbulent wake of the ahmed body. *Journal of Fluid Mechanics* **985**, A19.

Cherry, NJ, Hillier, R & Latour, MEMP 1984 Unsteady measurements in a separated and reattaching flow. *Journal of Fluid Mechanics* **144**, 13–46.

Duetsch-Patel, Julie E, MacGregor, Daniel, Jenssen, Yngve L, Henry, Pierre-Yves, Muthanna, Chittiappa, Savio, Luca, Lavoie, Philippe, Gargiulo, Aldo, Sundarraj, Vignesh, Ozoroski, Thomas A *et al.* 2022 The beverli hill three-dimensional separating flow case: cross-facility comparisons of validation experiment results. In *AIAA Scitech 2022 Forum*, p. 0698.

Duvvuri, Subrahmanyam & McKeon, Beverley J 2015 Triadic scale interactions in a turbulent boundary layer. *Journal of Fluid Mechanics* **767**, R4.

Eaton, John K & Johnston, James P 1982 Low frequency unsteadyness of a reattaching turbulent shear layer. In *Turbulent Shear Flows 3: Selected Papers from the Third International Symposium on Turbulent Shear Flows, The University of California, Davis, September 9–11, 1981*, pp. 162–170. Springer.

Fang, Xingjun & Wang, Zhan 2024 On the low-frequency flapping motion in flow separation. *Journal of Fluid Mechanics* **984**, A76.

Floc'h, Le, Suryadi, Alexandre, Hu, Nan, Herr, Michaela, Wang, Sen, Ghaemi, Sina, Vétel, Jérôme, Di Labbio, Giuseppe, Dufresne, Louis *et al.* 2024 Wall pressure signature of separated flows: A comparison between flat plate and airfoil .

Gray, Patrick D, Gluzman, Igal, Thomas, Flint, Corke, Thomas, Lakebrink, Matthew & Mejia, Kevin 2021 A new validation experiment for smooth-body separation. In *AIAA Aviation 2021 Forum*, p. 2810.

Gray, Patrick D, Gluzman, Igal, Thomas, Flint O, Corke, Thomas C, Lakebrink, Matthew T & Mejia, Kevin 2022 Benchmark characterization of separated flow over smooth gaussian bump. In *AIAA Aviation 2022 Forum*, p. 3342.

Klopsch, Roman, Fuchs, Lukas M, Rigas, Georgios, Oberleithner, Kilian & von Saldern, Jakob GR 2025 Spectral analysis of attached and separated turbulent flows over a gaussian-shaped bump. *arXiv preprint arXiv:2512.13582* .

Mabey, Dennis G 1972 Analysis and correlation of data on pressure fluctuations in separated flow. *Journal of Aircraft* **9** (9), 642–645.

Manohar, Kevin H, Annamalai, Hariprasad, Williams, Owen, Morton, Chris & Martinuzzi, Robert J 2026 Unsteadiness in turbulent separated flow over a three-dimensional gaussian bump. *arXiv preprint arXiv:2603.05765* .

Manohar, Kevin H, Williams, Owen, Martinuzzi, Robert J & Morton, Chris 2023 Temporal super-resolution using smart sensors for turbulent separated flows. *Experiments in Fluids* **64** (5), 101.

Manthripragada, Krithsanvith & Saxton-Fox, Theresa 2024 Relating skewness and fourier harmonics in low reynolds number wake flow. In *AIAA AVIATION FORUM AND ASCEND 2024*, p. 4191.

Mohammed-Taifour, Abdelouahab & Weiss, Julien 2016 Unsteadiness in a large turbulent separation bubble. *Journal of Fluid Mechanics* **799**, 383–412.

Rizzetta, Donald P & Garmann, Daniel J 2023 Arch vortex in flow over a three-dimensional gaussian bump. *AIAA Journal* **61** (11), 5176–5179.

Steinfurth, Ben, Cura, Carolina, Fuchs, Lukas, Von Saldern, Jakob GR, Oberleithner, Kilian & Weiss, Julien 2024 Low-frequency spanwise dynamics of a turbulent separation bubble. In *13th International Symposium on Turbulence and Shear Flow Phenomena (TSFP13)*.

Steinfurth, Ben, Li, Mogeng, Scarano, Fulvio & Weiss, Julien 2025 Three-dimensional low-frequency dynamics of a turbulent separation bubble. *Journal of Fluid Mechanics* **1019**, R4.

Weiss, Julien, Mohammed-Taifour, Abdelouahab & Schwaab, Quentin 2015 Unsteady behavior of a pressure-induced turbulent separation bubble. *AIAA Journal* **53** (9), 2634–2645.

Williams, Owen J, Annamalai, Hariprasad, Ozoroski, Thomas A, Roy, Christopher J & Lowe, Todd 2022 Comparison of hill-type geometries for the validation and advancement of turbulence models. In *AIAA SCITECH 2022 Forum*, p. 1032.

Williams, Owen J, Samuell, Madeline, Robbins, Matthew L, Annamalai, Hariprasad & Ferrante, Antonino 2021 Characterization of separated flowfield over gaussian speed-bump cfd validation geometry. In *AIAA Scitech 2021 Forum*, p. 1671.

Williams, Owen JH & Smits, Alexander J 2025 Asymmetries in nominally symmetric flows. *Annual Review of Fluid Mechanics* **57**.